ZrO2 on GaN metal oxide semiconductor capacitors via plasma assisted atomic layer deposition

P. von Hauff, A. Afshar, A. Foroughi-Abari, K. Bothe, K. Cadien, and D. Barlage

Citation: Applied Physics Letters **102**, 251601 (2013); doi: 10.1063/1.4812475
View online: http://dx.doi.org/10.1063/1.4812475
View Table of Contents: http://scitation.aip.org/content/aip/journal/apl/102/25?ver=pdfcov
Published by the AIP Publishing

ZrO_2 on GaN metal oxide semiconductor capacitors via plasma assisted atomic layer deposition

P. von Hauff,[1] A. Afshar,[2] A. Foroughi-Abari,[2] K. Bothe,[1] K. Cadien,[2] and D. Barlage[1,a)]
[1]*Department of Electrical and Computer Engineering, University of Alberta, Edmonton, Alberta T6G 2V4, Canada*
[2]*Department of Chemical and Materials Engineering, University of Alberta, Edmonton, Alberta T6G 2V4, Canada*

(Received 17 May 2013; accepted 9 June 2013; published online 25 June 2013)

ZrO_2 has been deposited on GaN by Atomic Layer Deposition. Multiple Metal-Oxide-Semiconductor Capacitors with 4.4 nm, 5.4 nm, and 8.5 nm of ZrO_2 oxide were fabricated with Cr electrodes. Capacitance measurements produce capacitance densities as high as 3.8 μF/cm^2. Current densities of 0.88 A/cm^2 at 1 V for the 4.4 nm oxides and hysteresis values of less than 6 mV were observed for the 5.8 nm oxide, indicating an interfacial D_{it} not greater than 6.4×10^{10} cm^2. Temperature dependent current measurements revealed no signature Poole-Frankel component. Comprehensive assessment of these measurements indicates a low defect density oxide formed on GaN with a low number of interface states. © *2013 AIP Publishing LLC*.
[http://dx.doi.org/10.1063/1.4812475]

Gallium nitride (GaN) is currently being pursued for high power and high frequency electronics. GaN provides wide band gap, high electron saturation velocity ($\upsilon s = 3.0 \times 10^7$ cm/s), and a high critical breakdown electric field (Ec = 4.2 MV/cm).[1] Creating a high quality dielectric-semiconductor interface is critical to create higher performance GaN based Metal Oxide Semiconductor Field Effect Transistors (MOSFETs) for power and RF electronics.[2–4] Recently a number of high-κ dielectrics have been investigated.[5–8] Metal Organic Chemical Vapor Deposited HfO_2 and ZrO_2 on GaN has shown comparable results.[9] ZrO_2 provides a high dielectric constant ($\varepsilon_r \sim 24$), a large band gap (5.8 eV), and sufficient band offsets (conduction band ~1.1 eV, valence band ~1.6 eV).[10] By using improved deposition and enhanced surface preparation techniques, it is possible to deposit low defect density oxides via Atomic Layer Deposition (ALD). The GaN/ZrO_2 interface was assessed through current, frequency dependent capacitance, and hysteresis measurements.

The GaN/sapphire template substrates were acquired from Kyma Technologies. These wafers consisted of a 5 μm thick N+ GaN layers grown via High Pressure Vapor Phase Epitaxy on a proprietary buffer layer and a sapphire substrate. Qualification measurements from the vendor indicate surface defects less than 5 cm^{-2} for a typical wafer. Capacitance-Voltage (C-V) measurements revealed a doping concentration of 10^{18} cm^{-3}. Compared with past work on GaN, the low defect density presented by the bulk should offer a lower defect oxide growth regardless of technique.

ZrO_2 was then deposited on GaN by ALD. Multiple Metal-Oxide-Semiconductor capacitors (MOSCAP) with 4.4 nm, 5.4 nm, and 8.5 nm of ZrO_2 oxide were fabricated with Cr electrodes. Capacitance measurements produce capacitance densities as high as 3.8 μF/cm^2. These results were obtained on a GaN wafer with a dopant density of ~10^{18} cm^{-3}. Current densities of 0.88 A/cm^2 at 1 V for the 4.4 nm oxides and hysteresis values of less than 6 mV were observed for the 5.8 nm oxide indicating an interfacial D_{it} not greater than 6.4×10^{10} cm^3. The flat-band voltage of the MOSCAP was measured to be 0.3 V regardless of thickness. This is consistent with the theoretical value that should be expected for a Cr gate electrode and GaN substrate with doping of 10^{18} cm^{-3}. Temperature dependent current measurements revealed no signature Poole-Frankel (PF) component. A comprehensive assessment of these measurements indicates a low defect density oxide formed on GaN with a low number of interface states.

Oxygen plasma pretreatment was preformed prior to film deposition which inhibited the formation of metallic-like bonds between Zr and Ga at the interface. These metallic bond formations manifest themselves as interface states in the oxide. Treating the GaN with oxygen plasma (PO_2) before deposition removes the nitrogen present at the surface as nitrous oxide. Column-V-oxide bonds are known to be responsible for pinning of the Fermi level through chemisorption of oxygen causing lattice deformations and semimetallic states at the interface.[11]

ZrO_2 was deposited on the substrate via ALD at temperature of 373 K and a chamber pressure of ~1 Torr.

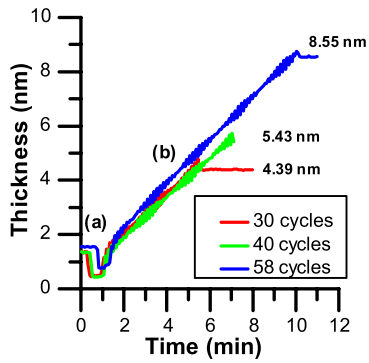

FIG. 1. The *in situ* ellipsometry data for each of the sample growths is shown. The pre-treatment in which the PO_2 is introduced coincides with the reduction in measured thickness.

a)Electronic mail: barlage@ualberta.ca

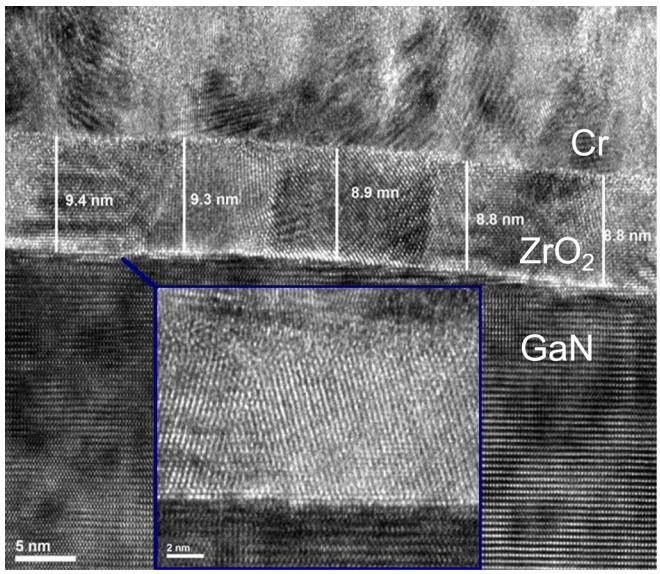

FIG. 2. TEM images revealed a well-defined ZrO_2/GaN interface. In the inset, the ZrO_2 appears poly-crystalline.

Alternating pulses of $Zr(NMe_2)_4$ and PO_2 were performed in a Kurt J. Lesker ALD150-L flow reactor with Argon as the carrier gas. The dose/purge duration for $Zr(NMe_2)_4$ and PO_2 was 0.04/5.0 s and 2.0/2.0 s, respectively. Plasma power was 600 W with a ramp of 6000 W/s. Before deposition, the substrates were exposed to a 30 s PO_2 for conditioning of the chamber and *in situ* cleaning of the surface. Based on the measured growth rates of ALD-ZrO_2 on silicon ⟨100⟩ wafers (~1.78 Å/cycle), 30, 40, and 58 cycles of ALD of ZrO_2 were grown on the GaN wafers. Fig. 1 shows *in situ* ellipsometry performed on the GaN template during deposition. The expected thicknesses using the ellipsometry data of the GaN templates were 4.4, 5.4, and 8.6 nm, respectively. We hypothesize that the pronounced dip observed in the thickness is the result of the removal of organic material from the GaN surface by the oxygen plasma that alters nucleation during early stages of growth. The later stages in the ellipsometry indicate the alternating precursor cycles resulting in a linear growth of the oxide. After ZrO_2 deposition, approximately 100 nm of Cr was deposited by magnetron sputtering. Once the contact metal was deposited, the templates were annealed at 688 K for 15 min.

High resolution Transmission Electron Microscopy (TEM) images of the thicker oxide were performed independently by

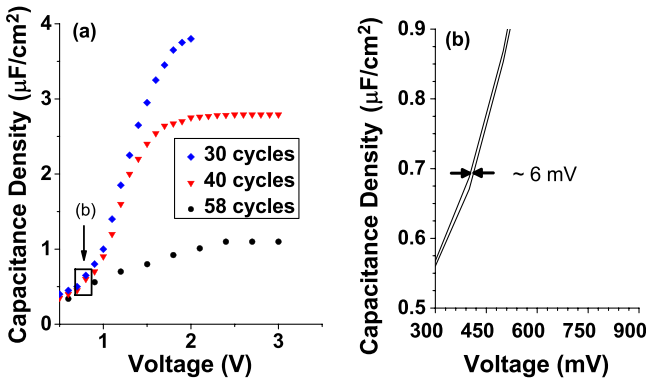

FIG. 4. (a) The typical Capacitance Density vs. Voltage (C-V) measurements of the MOSCAPs of the 30, 40, and 58 cycle samples. (b) The typical hysteresis in 40 cycle oxide.

Evans Analytical Group. As seen in Fig. 2, the TEM images revealed the 58 cycle sample oxide thickness was 9.1 ± 0.5 nm. The ellipsometry data were within error of the TEM. When calculating the resulting dielectric constants, each of these samples should have a systematic error of at least 0.5 nm based on the observed difference between ellipsometry and TEM data. The TEM images revealed that the PO_2 pretreatment created a well-defined ZrO_2/GaN interface and the oxide appeared crystalline rather than amorphous due to the observed well-ordered state of the ZrO_2.

The method of C-V dot fabrication and measurement is described previously.[12] The dopant density (N_D) and the flat-band voltage (V_{FB}) were calculated using ($1/C^2$-V), yielding 10^{18} cm^{-3} and 0.3 V, respectively. The theoretical (V_{FB}) was calculated using a nominal work function of 4.5 eV and 4.2 eV for Cr and GaN, producing a consistent (V_{FB})

$$V_{FB} = \phi_G - \left(\chi_S - \frac{kT}{q} \times \ln\left(\frac{N_{C(GaN)}}{N_D}\right)\right) - \frac{Q_{ox}}{C_{ox}}. \quad (1)$$

$N_{C(GaN)}$ was nearly equal to the N_D (2×10^{18} cm^{-3} vs. 1×10^{18} cm^{-3}), resulting in no significant difference in the Fermi level due to conduction band offset. (V_{FB}) was virtually invariant regardless of the oxide thickness. This provides supporting evidence of the absence of imbedded states in the oxide. Temperature dependent current vs. voltage (J-V) measurements were used to study oxide leakage and is shown in Fig. 3(a). Figs. 3(b) and 3(c) show the temperature dependent current (J-T) characteristics under negative and

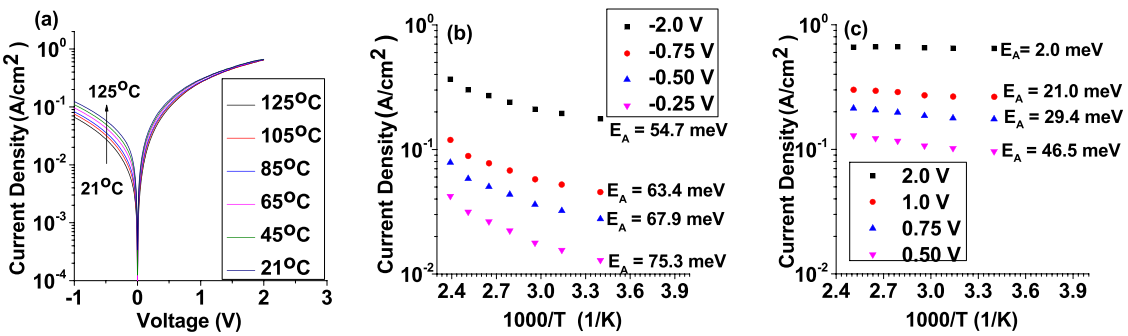

FIG. 3. (a) The temperature-dependent (J-V) characteristics for the MOSCAPs with 40 cycles of ZrO_2 deposited. (b) The temperature-dependent (J-T) characteristics with associated activation energies for a negative applied voltage. (c) The temperature-dependent (J-T) characteristics with associated activation energies with a positive applied voltage.

TABLE I. The experimental and theoretical oxide thickness, experimental and theoretical dielectric constant, hysteresis, capacitance, and traps are for the MOSCAPs.

t_{ox} (nm)(ellipsometry)	C_{ox} (μF/cm^2)	t_{acc} (nm)(assumed)	ε_r (ZrO_2)(calculated)	t_{acc} (nm) (calculated)	ε_r (ZrO_2) (assumed)	Hysteresis(mV)	D_{it} (hysteresis)
4.4 ± 0.5	3.8	1.0	34 ± 4	0.44 ± 0.05	24	20	2.0×10^{11}
5.4 ± 0.5	2.6	1.0	24 ± 2	1.0 ± 0.08	24	6	3.2×10^{10}
8.5 ± 0.5	1.1	1.0	13 ± 1	3.6 ± 0.06	24	30	6.4×10^{10}

positive bias found by using relation (1). The activation energies (EA) determined by fitting the linear regression observed in the (J-T) in forward bias plot near V_{FB}

$$E_A = \frac{\Delta \ln(J)}{\Delta \frac{1}{kT}}. \quad (2)$$

Fig. 3(b) shows the temperature dependent current (J-T) characteristics under negative biases. In reverse bias the leakage is from one of two mechanisms, i.e., electrons coming from the gate traveling to the body or holes tunneling from the body to gate. Given the small intrinsic carrier concentration and light isolated measurement conditions, it is unlikely that hole transport mechanisms are present. More likely the electrons make their way from the gate to available deep level donor states in the depleted GaN and subsequently are thermally activated to the conduction band. The reverse bias activation energy (75 meV-55 meV) would correspond to these states that are presumably in the depleted bulk GaN. In the forward bias, Fig. 3(c) shows at near (V_{FB}) the temperature dependent component comes from the shallow donor activation. From 0.5 V to 0.75 V this activation energy ranges from 30 to 21 meV which is consistent with the accepted donor (E_A) of 22 meV for Si in GaN.[13] In strong accumulation we observe virtually no change in current with respect to temperature ($E_A = 2$ meV). The low (E_A) is consistent with oxides only exhibiting direct or Fowler Nordheim tunneling currents. A large activation energy ($E_A > 150$ meV) in the (J-T) relation would be consistent with the conduction band offsets in the dielectric material if defect assisted thermal emission, PF, were present. The samples were measured under an extensive set of conditions for the temperature range described. Under no circumstance was a large activation energy observed; thus, we conclude that minimum numbers of defects are present in the oxide.

Fig. 4(a) represents the amalgamation of (C-V) measurements performed from 1 KHz to 1 MHz. The raw data were processed through transformation of a circular distributed capacitance model.[14] The 58, 40, 30 cycle samples displayed a peak capacitances of 1.1 μF/cm^2, 2.7 μF/cm^2, and. 3.8 μF/cm^2, respectively, and were analyzed using the following relation:

$$C_{ox} = \varepsilon_o \left(\frac{t_{ox}}{\varepsilon_r(ZrO_2)} + \frac{t_{acc}}{\varepsilon_r(GaN)} \right)^{-1}. \quad (3)$$

The results are summarized in Table I with alternative analyses. If (ε_r) is forced to be 24 and the accumulation layer is allowed to vary, we create an unphysical situation where the accumulation layer would be unrealistically small for the applied electric field. It is far more likely that the accumulation layer maintains a constant value of approximately 1.0 nm for constant electric field. An accumulation layer thickness of 1.0 nm is consistent with the expected thickness of the electron gas in GaN that we determined by examining the accumulation layer thickness for the well known materials of SiO_2 and AlGaN on GaN using a commercial (Synopsis) 2D Poison-Schrodinger solver. These were chosen for simulation because the effective masses of these material systems are well known. In the ZrO_2 case, an electron effective mass ratio is still not widely agreed upon, but the value should lie between the value of SiO_2 and the value of AlGaN. The method of solution has been previously described for silicon,[15] and some of the results for this analysis are included in the supplementary material.[17] The centroid of simulated accumulation layer charge was typically 1.3-1.5 nm for SiO_2 and 0.75-0.95 nm for AlGaN for a large range of total charge in deep accumulation. No low frequency, abnormally large conductance was observed in the experimental results indicating that the enhanced dielectric constant was not an artifact of trap states. Furthermore the *in situ* ellipsometry indicates that no obvious difference in the interface is present and should resemble the interface presented in the TEM. This leads to the observation that (ε_r) of the material actually increases with decreasing thickness.

The hysteresis in the (C-V) measurements was 6 mV at 20 KHz (Fig. 4(b)) and was consistent at multiple frequencies and temperatures. Using a commonly used method,[16] the D_{it} for the MOS capacitor with 40 cycle of ZrO_2 was estimated as 3.2×10^{10} eV^{-1} cm^{-2}. This was repeated for all thicknesses and is summarized in the Table I. While extraneous sources of hysteresis were minimized by the careful shorting of the surrounding dielectric and the low defect starting material provided by Kyma, there is a residual substrate charging effect that will add to the measurement of the D_{it} but not be physically present in the actual interface. The reported values should be taken as a worse case measurement of interface traps.

The authors would like to thank Alberta Innovates, the NSERC discovery grant program, and the University of Alberta Faculty of Engineering for supporting this work.

[1]A. M. Ozbek and B. J. Baliga, IEEE Electron Device Lett. **32**(10), 300–302 (2011).
[2]K. Bothe, M. A. L. Johnson, and D. W. Barlage, in *CS MANTECH Conference*, 2011.
[3]W. Huang, T. Khan, and T. P. Chow, in *Proceedings of the 18th International Symposium on Power Semiconductor Devices & IC's, 4–8 June 2006*, pp. 1–4.
[4]K. Matocha, T. P. Chow, and R. J. Gutmann, IEEE Trans. Electron Devices **52**(1), 6–10 (2005).
[5]Y. C. Chang, H. C. Chiu, Y. J. Lee, M. L. Huang, K. Y. Lee, M. Hong, Y. N. Chiu, J. Kwo, and Y. H. Wang, Appl. Phys. Lett. **90**(23), 232904 (2007).

[6]H. Cho, K. P. Lee, B. P. Gila, C. R. Abernathy, S. J. Pearton, and F. Ren, Solid State Electron. **47**(10), 1757–1761 (2003).
[7]J. W. Johnson, B. Luo, F. Ren, B. P. Gila, W. Krishnamoorthy, C. R. Abernathy, S. J. Pearton, J. I. Chyi, T. E. Nee, C. M. Lee, and C. C. Chuo, Appl. Phys. Lett. **77**(20), 3230–3232 (2000).
[8]J. S. Jur, V. D. Wheeler, M. T. Veety, D. J. Lichtenwalner, D. W. Barlage, and M. A. L. Johnson, in *CS MANTECH Conference*, 2008.
[9]S. Abermann, G. Pozzovivo, J. Kuzmik, G. Strasser, D. Pogany, J.-F. Carlin, N. Grandjean, and E. Bertagnolli, Semicond. Sci. Technol. **22**, 1272–1275 (2007).
[10]J. Robertson and B. Falabretti, J. Appl. Phys. **100**, 014111 (2006).
[11]M. J. Hale, S. I. Yi, J. Z. Sexton, A. C. Kummel, and M. Passlack, J. Chem. Phys. **119**(13), 6719–6728 (2003).
[12]P. von Hauff, K. Bothe, A. Afshar, A. Foroughi-Abari, D. Barlage, and K. Cadien, in *CS MANTECH, Boston Massachusetts, May* 2012.
[13]M. Leroux, N. Grandjean, B. Beaumont, G. Nataf, and F. Semond, J. Appl. Phys. **86**, 3721 (1999).
[14]K. Bothe, P. A. von Hauff, A. Afshar, A. Foroughi-Abari, K. C. Cadien, and D. W. Barlage, IEEE Trans. Electron Devices **59**, 2662–2666 (2012).
[15]S. A. Hareland, S. Krishnamurthy, S. Jallepalli, C.-F. Yeap, K. Hasnat, A. F. Tasch, Jr., and C. M. Maziar, IEEE Trans. Electron Devices **43**, 90–96 (1996).
[16]S. C. Witczak, J. S. Suehle, and M. Gaitan, Solid State Electron. **35**, 345–355 (1992).
[17]See supplementary material at http://dx.doi.org/10.1063/1.4812475 for a brief description of results and methods for determination of charge centroid.